

# Evolution of surface vanadia-like species on unsupported V–O–W catalyst for NO decomposition in the course of redox-treatment

A. Białas<sup>a</sup>, B. Borzęcka-Prokop<sup>a</sup>, A. Weselucha-Birczyńska<sup>b</sup>, J. Camra<sup>b</sup>, M. Najbar<sup>a,\*</sup>

<sup>a</sup> Department of Chemistry, Jagiellonian University, Ingardena 3, 30060 Kraków, Poland

<sup>b</sup> Regional Laboratory of Physicochemical Analyses and Structural Research, Jagiellonian University, Ingardena 3, 30060 Kraków, Poland

Available online 8 September 2006

## Abstract

The evolution of surface species on unsupported V–O–W catalyst (V:W = 2:9) as a result of its oxidizing and reducing thermal treatments was investigated. The catalyst was prepared by annealing an oxalate precursor at 773 K in air for 1 h and then subjected to further oxidizing or reducing thermal treatments. It was revealed using XRD that the freshly prepared catalyst contains mainly the crystallites of the tetragonal phase of V–W oxide bronze which transforms into monoclinic WO<sub>3</sub> during further annealing due to surface vanadium segregation. XPS results showed that in the surface nanolayers of the freshly prepared catalyst vanadium occurs mostly as vanadium suboxides species. Raman spectroscopy results revealed mostly crystalline vanadia-like species as well as monolayer vanadia-like species on the freshly prepared catalyst. Essential changes in the structure of the vanadia-like species as a result of the catalyst thermal treatments were observed. The thermal treatment in the oxidizing atmosphere caused an increase in the content of the crystalline vanadia-derived surface species—that did not contain tungsten in their structure. Monolayer species with relatively high tungsten content were formed during the catalyst thermal treatment in reducing conditions.

© 2006 Elsevier B.V. All rights reserved.

**Keywords:** V–O–W oxide bronze; Surface V segregation; Vanadia-like surface species

## 1. Introduction

Vanadia can occur on the surface of a support as monomers, polymers or crystallites depending on its concentration [1,2]. According to Went et al. [2], polymeric V<sub>2</sub>O<sub>5</sub> is 10 times more active in selective NO reduction with ammonia (NH<sub>3</sub>–SCR of NO) than monomeric vanadia. However, monomeric species show higher and independent of oxygen presence selectivity towards N<sub>2</sub> [2]. Wachs et al. observed similar changes in catalyst activity and selectivity with vanadia loading [3]. Haber et al. [4] postulated that side faces of the crystalline surface vanadia species are mostly responsible for NH<sub>3</sub>–SCR of NO.

The addition of tungsta increases catalyst activity, widens the temperature window—lowers the temperature of initial activity and enhances the temperature of the final activity, increases catalyst resistance to poisoning by alkali and arsenic [5,6]. The content of WO<sub>3</sub> in such ternary catalysts is about

10 wt.% and the content of V<sub>2</sub>O<sub>5</sub> was 1–2 wt.% [7]. The presence of WO<sub>3</sub> also enhances the thermal stability of the catalyst thanks to good crystallographic matching between TiO<sub>2</sub> and WO<sub>3</sub> as well as WO<sub>3</sub> and V<sub>2</sub>O<sub>5</sub> [8]. WO<sub>3</sub> prevents sintering anatase as well as the transformation of anatase into rutile [9]. It is also stated that in those ternary catalysts vanadia species are responsible for DeNO<sub>x</sub> activity [10]. Paganini et al. [11] have explained the influence of tungsten by the changes that occur in electronic properties of the system, tungsten has not been regarded to cause the phase transformation. Our earlier investigation [12] revealed that tungsten oxide and vanadium oxide form V–W oxide bronze with the structure described earlier for W–Na oxidic bronze [13]. Bronze annealing at temperatures higher than the obtainment temperature results in partial segregation of bronze compounds along with formation of monoclinic WO<sub>3</sub> and surface vanadia-like species. A structural investigation of surface species complemented by quantum-mechanical calculations by DFT method [14,15] allows us to state that vanadia-like species with some W<sup>6+</sup> atoms substituted for vanadium ones form on the surface of monoclinic WO<sub>3</sub> crystallites. In such species adjacent V<sup>5+</sup> ions

\* Corresponding author.

E-mail address: [mnajbar@chemia.uj.edu.pl](mailto:mnajbar@chemia.uj.edu.pl) (M. Najbar).

are reduced to  $V^{4+}$  ones. It was found that crystallographic matching between vanadia-like species and monoclinic tungsta is better than among those species and  $TiO_2$  supports [16]. Najbar et al. [17] showed that surface species on unsupported V–O–W catalyst (W:V = 9:1) are present as monolayer and crystalline ones.

The aim of this paper is to investigate the effect of temperature, time and the atmosphere of annealing on the population and structure of surface species formed on crystallites of oxide V–W bronze as a result of vanadium segregation. We expect that results of these studies could help us to design a V–O–W catalyst surface for different types of reactions;  $NH_3$ –SCR of NO with ammonia as well as organic syntheses based on oxidation [18,19] and ammoxidation of hydrocarbons [20].

## 2. Experimental

Mixed vanadium-tungsten oxide was obtained from ammonium salts  $(NH_4)_{10}W_{12}O_{41} \cdot 5H_2O$  and  $NH_4VO_3$ . Ammonium methavanadate and ammonium polytungstate (V:W = 2:9) were dissolved separately in saturated oxalic acid, then the solutions were mixed and evaporated under stirring. After drying at 353 K the catalyst was obtained from the precursor by annealing it at 773 K in air for 1 h. Then the catalyst was annealed at (a) 673 K, for 115 h, (b) 673 K in a vacuum ( $3.3 \times 10^{-3}$  Pa) for 14 h and (c) 773 K in air for 2 h. A separate portion of the catalyst precursor was annealed at 793 K in air for 3 h.

The phase composition of the catalysts was examined by powder XRD. A Philips Analytical PW 3710 XPERT System with Cu K $\alpha$  ( $\lambda = 0.1541$  nm) radiation (40 kV, 30 mA) and secondary beam monochromator at  $0.02^\circ$  steps at the rate of 2 s per step over the range  $10 < 2\theta < 30$  was used to record patterns.

The chemical composition of the catalyst surface nanolayers was determined by X-ray photoelectron spectroscopy (XPS). XPS spectra were measured using an ESCA 150 spectrometer (VSW Scientific Instruments) with a magnesium anode as a source of X-ray, a hemispherical analyser 150 mm in diameter and Leybold multichannel detector.

The structure of the surface species was determined by FT Raman spectroscopy. A BIO-RAD FT Raman spectrometer with Spectra Physics Nd:YAG Laser with excitation line 1064 nm was used. The sampling width was  $2\text{ cm}^{-1}$ .

## 3. Results and discussion

In Fig. 1, XRD patterns of the V–O–W catalysts: (A) freshly prepared, (B) annealed at 673 K, for 115 h, (C) annealed at 773 K in air for 2 h and (D) obtained at 793 K, are presented in the range  $2\theta = 10\text{--}30^\circ$  (T: tetragonal V–W oxide bronze; M: monoclinic  $WO_3$ ). In the XRD pattern of the freshly prepared catalyst strong reflections of the tetragonal V–W oxide bronze, weaker ones of monoclinic  $WO_3$ , and very weak ones of vanadia were detected. The comparison of the XRD patterns of the freshly prepared and thermally treated catalysts indicates the formation of monoclinic  $WO_3$  and  $V_2O_5$  at the cost of the

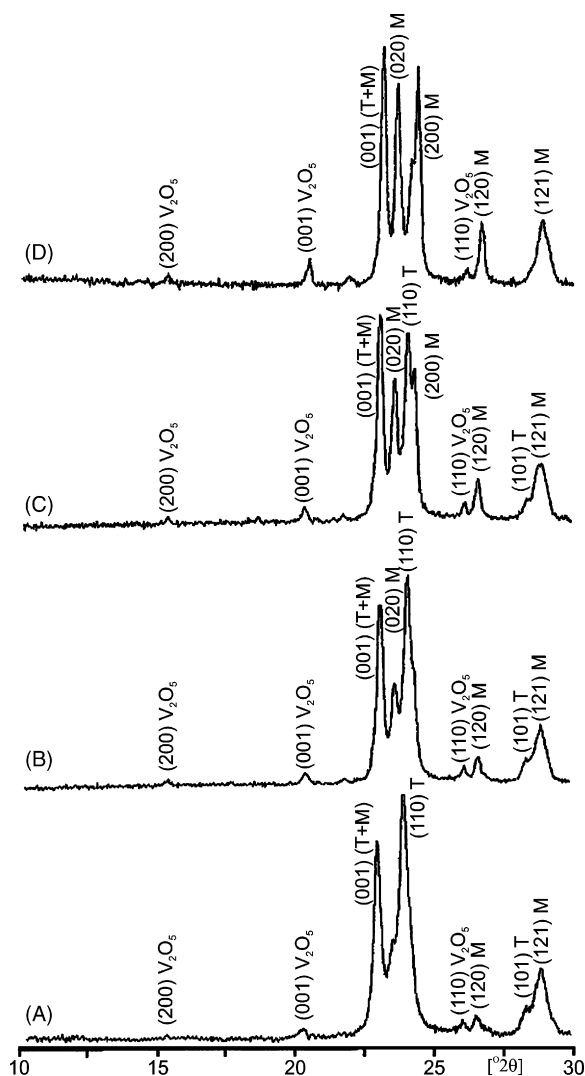


Fig. 1. XRD patterns of V–O–W catalysts: (A) freshly prepared by precursor annealing at 773 K in air for 1 h, (B) annealed at 673 K for 115 h, (C) annealed at 773 K in air for 2 h and (D) obtained by precursor annealing at 793 K in air for 3 h,  $2\theta = 10\text{--}30^\circ$ ; T: tetragonal V–W oxide bronze; M: monoclinic  $WO_3$ .

tetragonal V–W oxide bronze in the course of the catalyst thermal treatments. The amount of monoclinic  $WO_3$  formed increases as the temperature of the thermal treatment increases. In the catalyst obtained at 793 K in air almost all tungsta occurred in the monoclinic form and the quantity of vanadia is the highest.

Fig. 2 presents XPS spectra in the  $V2p_{3/2}$  band range of V–O–W catalysts: (A) freshly prepared, (B) annealed at 673 K for 115 h, (C) annealed at 673 K in a vacuum ( $3.3 \times 10^{-3}$  Pa) for 14 h, (D) annealed at 773 K in air for 2 h, (E) obtained at 793 K. Using the XPS-peak program [21],  $V2p_{3/2}$  bands were deconvoluted into three peaks corresponding to  $V_2O_5$ ,  $V_2O_4$  and  $V_2O_3$ . Table 1 presents binding energies of the particular V species and  $N_V/N_W$  ratio—calculated from  $V2p_{3/2}$  and  $W4f_{7/2}$  peaks. As seen in Table 1, in the freshly prepared catalyst most of vanadium (58.3%) is present as  $V^{4+}$  species, about one third (32.1%) as  $V^{3+}$  and 9.6% as entirely oxidized  $V^{5+}$  species.

During the process of annealing in air at 673 K for 115 h (Fig. 2B)  $N_V/N_W$  ratio increased from 0.19 to 0.24 and the

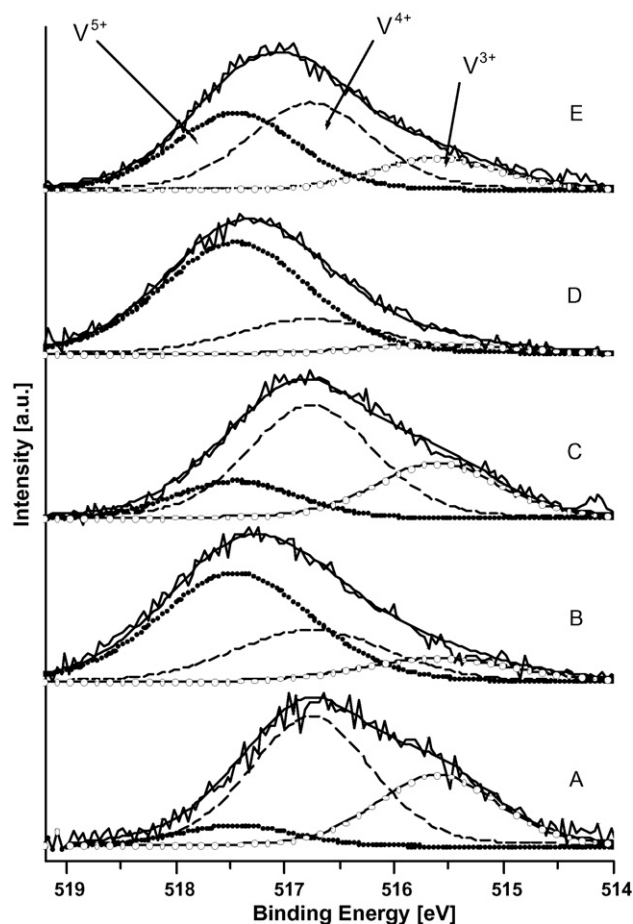


Fig. 2. XPS spectra in the  $V2p_{3/2}$  band range of V–O–W catalysts: (A) obtained by precursor annealing at 773 K in air for 1 h, (B) annealed at 673 K in air for 115 h, (C) annealed at 673 K in a vacuum ( $3.3 \times 10^{-3}$  Pa) for 14 h, (D) annealed at 773 K in air for 2 h and (E) obtained by precursor annealing at 793 K in air for 3 h.

oxidation state of vanadium increased as well. The content of  $V^{5+}$  species increased to 59.2% at the cost of the lowering of the  $V^{4+}$  and  $V^{3+}$  species contents to 28.1 and 12.7%, respectively. Taking into account that crystallinity of surface vanadium species did not decrease and the content of the V–W oxide bronze decreased (Fig. 1A and B), the increase of the vanadium content in the surface nanolayer should be ascribed to the surface vanadium segregation.

The annealing in vacuum also caused the  $N_V/N_W$  ratio to increase and an unexpected increase of the oxidation state of V ions. The increased  $N_V/N_W$  ratio shows further surface

vanadium segregation from bronze crystallites. However, the slight increase of the vanadium oxidation state shows that vacuum conditions are less reducing than those of the synthesis. It should be remembered that during oxalate precursor annealing, strongly reducing CO evolves. The higher value of the  $N_V/N_W$  ratio for the catalyst annealed at 673 K in vacuum than that of the catalyst annealed for much longer (115 h) at the same temperature in air clearly shows the formation of vanadia-like crystallites with dimension larger than the depth of microprobe analysis in oxidizing conditions and the formation of monolayer species in reducing ones.

Thermal treatment at 773 K in air for 2 h caused the strongest oxidation of the V species. The  $V^{5+}$  content achieved 71.70% and contents of  $V^{4+}$  and  $V^{3+}$  decreased to 22 and 6.3%, respectively. Unlike the great differences in XRD patterns of the catalysts annealed at 673 and 773 K in air, the  $N_V/N_W$  ratios are almost the same for both catalysts. This disparity may be easily explained by the formation of the larger vanadia-like crystallites during the annealing at 773 K than those formed at 673 K (compare Fig. 1B and C). It is thus clear that an oxidizing atmosphere and relatively high temperature are favourable for the surface vanadia-like crystallites growth.

The catalyst precursor thermal treatment at 793 K causes the biggest increase in the  $N_V/N_W$  ratio. Inversely, the increase of the catalyst precursor thermal treatment to 793 K yields a catalyst with V species with a relatively low degree of oxidation. This suggests that at this temperature vanadia-like surface species undergo partial decomposition due to the higher value of equilibrium oxygen pressure above them than the partial oxygen pressure in air at this temperature.

Fig. 3 presents Raman spectra of V–O–W catalysts: (A) freshly prepared, (B) annealed at 673 K in air for 115 h, (C) annealed at 673 K in a vacuum ( $3.3 \times 10^{-3}$  Pa) for 14 h, (D) annealed at 773 K in air for 2 h and (E) obtained by the precursor annealing at 793 K in air for 3 h, in the lattice vibration range—100–165  $\text{cm}^{-1}$ .

In the spectrum of the freshly prepared catalyst (Fig. 3A), the band at 145  $\text{cm}^{-1}$  from a  $V_2O_5$  crystalline phase as well as shoulders at 116 and 125  $\text{cm}^{-1}$  typical of tetragonal oxidic tungsten bronze [22] are present. Shoulders at 155 and 162  $\text{cm}^{-1}$  can be ascribed to the lower vanadium oxides— $V_2O_4$  and  $V_4O_9$ , respectively [23]. Further annealing of the sample, at 673 K for 115 h (Fig. 3B), led to almost complete disappearance of shoulders from oxidic tungsten bronze and from lower vanadium oxides. Only peaks from monoclinic

Table 1  
Binding energies of the  $V^{5+}$ ,  $V^{4+}$ ,  $V^{3+}$  species and  $N_V/N_W$  ratio—calculated from  $V2p_{3/2}$  and  $W4f_{7/2}$  peaks

Catalyst	$V2p_{3/2}$			$N_V/N_W$
	$V^{5+}$ (517.45 eV) (%)	$V^{4+}$ (516.75 eV) (%)	$V^{3+}$ (515.60 eV) (%)	
Freshly prepared	9.6	58.3	32.1	0.19
Annealed at 673 K for 115 h	59.2	28.1	12.7	0.24
Annealed at 673 K in a vacuum ( $3.3 \times 10^{-3}$ Pa) for 14 h	18.4	54.9	26.7	0.25
Annealed at 773 K in air for 2 h	71.7	22.0	6.3	0.25
Precursor annealed at 793 K in air for 3 h	38.3	42.7	19.0	0.28

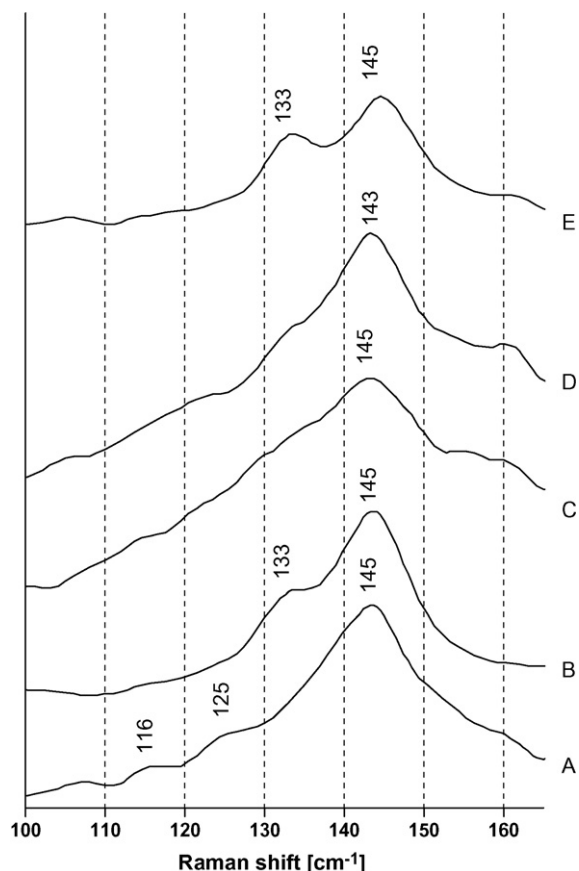


Fig. 3. Raman spectra of V–O–W catalysts: (A) freshly prepared, (B) annealed at 673 K in air for 115 h, (C) annealed at 673 K in a vacuum ( $3.3 \times 10^{-3}$  Pa) for 14 h, (D) annealed at 773 K in air for 2 h and (E) obtained by precursor annealing at 793 K in air for 3 h in the lattice vibration range of 100–165  $\text{cm}^{-1}$ .

$\text{WO}_3$ —133  $\text{cm}^{-1}$  and crystalline  $\text{V}_2\text{O}_5$  are distinctly visible. It can thus be concluded that the catalyst annealing at 673 K in air for 115 h leads to vanadium segregation from the bronze crystallites' nanolayers, which results in the transformation of the bronze phase into monoclinic tungsta one. However, crystalline surface species of lower vanadium oxide structure undergo oxidation and become vanadia ones. It is obvious that the total amount of surface vanadia-like species increases, which is illustrated by the XPS results in Table 1.

Thermal treatment at 673 K in a vacuum ( $3.3 \times 10^{-3}$  Pa) for 14 h (Fig. 3C), causing enrichment of the catalyst surface nanolayers in vanadium (Table 1), did not lead to the monoclinic tungsta peak appearance in the spectrum. This suggests that segregated vanadium remained in the bronze layer as surface or subsurface add-atoms. It is also possible that such vanadium add-atoms are formed as a result of the reduction of vanadia-derived species on the boundary with tungsta. However, the reduction of the surface species resulting from the formation of the lower, dark coloured vanadium oxide decreases the thickness of the layer analyzed by Raman spectroscopy and therefore the lack of a monoclinic tungsta peak does not necessarily show a lack of this phase in non-analysed sub-surface layers.

Annealing at 773 K for 3 h in air (Fig. 3D) caused progressive surface vanadium segregation from tungsten bronze (appearance of the monoclinic tungsta peak and

lowering of the intensity of bronze peaks) and oxidation of the  $\text{V}_2\text{O}_4$ -like species. Raising the annealing temperature to 793 K brought about the crystallisation of monoclinic  $\text{WO}_3$  and  $\text{V}_2\text{O}_5$  (Fig. 3E).

Fig. 4 shows Raman spectra of V–O–W catalysts: (A) freshly prepared, (B) annealed at 673 K, for 115 h, (C) annealed at 673 K in a vacuum ( $3.3 \times 10^{-3}$  Pa) for 14 h, (D) annealed at 773 K in air for 3 h and (E) 793 K in air for 3 h; in the range of  $\text{V}=\text{O}$  stretching vibrations—850–1050  $\text{cm}^{-1}$ .

In the spectrum of the freshly prepared catalyst (Fig. 4A), the peak at 991  $\text{cm}^{-1}$  – typical of crystalline  $\text{V}_2\text{O}_5$  – is accompanied by peaks at 974 and 968  $\text{cm}^{-1}$  and the shoulder at 870  $\text{cm}^{-1}$ . The first of the peaks was earlier ascribed to the vanadia-like monolayer [17,24] and the second one to  $\text{V}=\text{O}$  in the neighborhood of the tungsten atom in the  $\text{V}_2\text{O}_5$  lattice [14] and the shoulder at 870  $\text{cm}^{-1}$  to  $\text{W}=\text{O}$  in the vanadia lattice [14]. We can thus conclude that in addition to crystalline (Fig. 4) monolayer species are present at the surface of V–W oxide bronze crystallites of the freshly prepared catalyst.

Additional annealing at 673 K, for 115 h (Fig. 4B) led to the growth of crystalline  $\text{V}_2\text{O}_5$  due to surface vanadium segregation

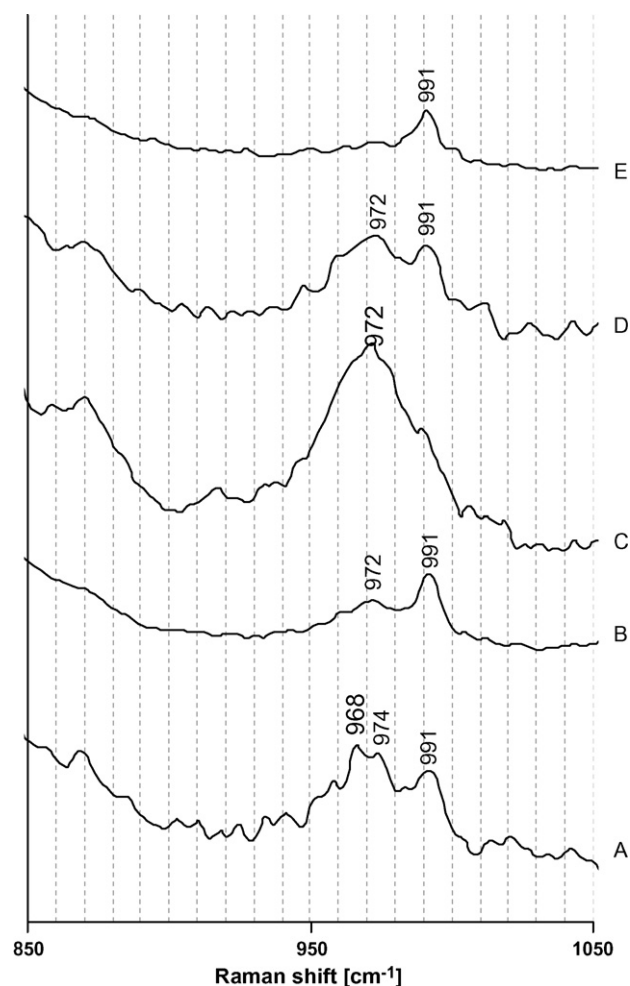


Fig. 4. Raman spectra of V–O–W catalysts: (A) freshly prepared, (B) annealed at 673 K for 115 h, (C) annealed at 673 K in a vacuum ( $3.3 \times 10^{-3}$  Pa) for 14 h, (D) annealed at 773 K in air for 2 h and (E) obtained by annealing at 793 K in air for 3 h; in the range of 850–1050  $\text{cm}^{-1}$ .



and monolayer diminishment. The disappearance of the peak at ca 870  $\text{cm}^{-1}$  clearly illustrates that tungsten is present mostly in the structure of monolayer vanadia-like species.

Thermal treatment in a vacuum (Fig. 4C) leads mostly to monolayer vanadia-derived surface species enriched in tungsten.

Further annealing –2 h, at 773 K in air does not cause distinct changes in the relation between monolayer and crystalline vanadia-derived species (Fig. 4D).

In the catalyst obtained at 793 K only crystalline pure  $\text{V}_2\text{O}_5$  and monoclinic tungsta are present (Fig. 4E). It suggests that both phases crystallized separately.

#### 4. Conclusions

Evolution of the surface and the bulk of the unsupported V–O–W catalyst (V:W = 2:9) as a result of its oxidizing and reducing thermal treatments were investigated to gain the information necessary to design the structure of the surface species and to understand species transformations in the course of the  $\text{NH}_3$ –SCR of NO.

The catalyst precursor was obtained from vanadyl and tungsten oxalates. It was transformed into the catalyst in the course of annealing at 773 K in air for 1 h. The catalyst was then subjected to oxidation at 673 or 773 K in air and to reduction at 673 K in a vacuum. The freshly prepared, oxidized and reduced samples of the catalyst were investigated by XRD, XPS and Raman spectroscopy. It was revealed that the freshly prepared catalyst is composed mostly of the crystallites of the tetragonal V–W oxide bronze covered by crystalline and monolayer vanadia-like species. Annealing in an oxidizing atmosphere was shown to cause surface vanadium segregation resulting in V–W oxide bronze transformation into monoclinic tungsta accompanied by surface vanadia-derived crystalline species formation. However, annealing in a reducing atmosphere resulted mostly in monolayer vanadia-derived species formation on the surface of the V–W oxide bronze crystallites. The high content of tungsten was revealed in the monolayer vanadia-derived species and tungsten was practically absent in

crystalline species, which suggests crystallite growth via gas phase transportation.

#### References

- [1] G.T. Went, L.-J. Leu, A.T. Bell, *J. Catal.* 134 (1992) 479.
- [2] G.T. Went, L.-J. Leu, R.R. Rosin, A.T. Bell, *J. Catal.* 134 (1992) 492.
- [3] I.E. Wachs, G. Deo, B.M. Weckhuysen, A. Andreini, M.A. Vuurman, M. Boer, M. Amiridis, *J. Catal.* 161 (1996) 211.
- [4] M. Gąsior, J. Haber, T. Machej, T. Czeppe, *J. Mol. Catal.* 43 (1988) 359.
- [5] J.P. Chen, R.T. Yang, *Appl. Catal. A* 80 (1992) 135.
- [6] L.J. Alemany, F. Berti, G. Busca, G. Ramis, D. Robba, G.P. Toledo, M. Trombetta, *Appl. Catal. B: Environ.* 10 (1996) 299.
- [7] L.J. Alemany, L. Lietti, N. Ferlazzo, P. Forzatti, G. Busca, E. Giamello, F. Bregani, *J. Catal.* 155 (1995) 117.
- [8] M. Najbar, F. Mizukami, in: *Proceedings of Second Polish Seminar on Catalytic DENOX*, Rabka, November 27–28, (1995), p. 21.
- [9] C. Cristiani, M. Bellotto, P. Forzatti, F. Bregani, *J. Mater. Res.* 8 (1993) 2019.
- [10] G. Busca, L. Lietti, G. Ramis, F. Berti, *Appl. Catal. B: Environ.* 18 (1998) 1.
- [11] M.C. Paganini, L. Dall'Acqua, E. Giamello, L. Lietti, P. Forzatti, G. Busca, *J. Catal.* 166 (1997) 195.
- [12] M. Najbar, J. Camra, A. Białas, A. Weselucha-Birczyńska, B. Borzęcka-Prokop, L. Delevoye, J. Klinowski, *Phys. Chem. Chem. Phys.* 1 (1999) 4645.
- [13] L. Bartha, A.B. Kiss, T. Szalay, *Int. J. Refractory Met. Hard Mater.* 13 (1995) 77.
- [14] M. Najbar, E. Broclawik, A. Góra, J. Camra, A. Białas, A. Weselucha-Birczyńska, *Chem. Phys. Lett.* 325 (2000) 330.
- [15] E. Broclawik, A. Góra, M. Najbar, *J. Mol. Catal.* 166 (2001) 31.
- [16] M. Najbar, F. Mizukami, M. Izutsu, *Pol. J. Environ. Studies* 9 (2000) 45.
- [17] M. Najbar, F. Mizukami, P. Kornelak, A. Weselucha-Birczyńska, B. Borzęcka-Prokop, E. Bielańska, A. Białas, J. Banaś, D. Su, *Catal. Today* 90 (2004) 93.
- [18] A. Satsuma, F. Okada, A. Hattori, A. Miyamoto, T. Hattori, Y. Murakami, *Appl. Catal.* 72 (1991) 295.
- [19] Z. Yan, S.L.T. Andersson, *Appl. Catal.* 66 (1990) 149.
- [20] US Patent 3,312,710 (1967).
- [21] XPS Table, [www.lasurface.com](http://www.lasurface.com).
- [22] M. Najbar, A. Białas, A. Weselucha-Birczyńska, in: *Proceedings of the Third International Conference Catalysis and Adsorption In Fuel Processing and Environmental Protection*, Wrocław, (1999), p. 427.
- [23] Y. Zhang, M. Meisel, A. Martin, B. Lucke, K. Witke, K.W. Brzezinka, *Chem. Mater.* 9 (1997) 1086.
- [24] J. Banaś, V. Tomasic, A. Weselucha-Birczyńska, M. Najbar, *Catal. Today*, this issue.